

Electronic Supplementary Information (ESI)

3D printed SrNbO₂N photocatalyst for degradation of organic pollutants in water

Antonio Iborra-Torres^a, Matej Huš^{b,c,d}, Kiem Nguyen^e, Antonis Vamvakeros^{f,g}, Muhammad Tariq Sajjad^e, Steven Dunn^e, Myrjam Mertens^h, Simon Jacques^f, Andrew M. Beale^{f,g,i}, Blaž Likozar^b, Geoffrey Hyett^a, Suela Kellici^e, Vesna Middelkoop^{h*}

^a Department of Chemistry, University of Southampton, Southampton, SO17 1BJ, United Kingdom

^b Department of Catalysis and Chemical Reaction Engineering, National Institute of Chemistry, SI-1001 Ljubljana, Slovenia

^c Association for Technical Culture of Slovenia, Zaloška 65, SI-1001 Ljubljana, Slovenia

^d Research Institute, Conservation Centre, Institute for the Protection of Cultural Heritage of Slovenia, Poljanska 40, SI-1000 Ljubljana, Slovenia

^e London Centre for Energy Engineering, School of Engineering, London South Bank University, London SE1 0AA, United Kingdom

^f Finden, Building R71, Harwell Campus, Oxfordshire, OX11 0QX, United Kingdom

^g Department of Chemistry, University College London, London WC1H 0AJ, United Kingdom

^h Sustainable Materials Management, Flemish Institute for Technological Research (VITO), B-2400 Mol, Belgium

ⁱ Research Complex at Harwell, Rutherford Appleton Laboratory, Harwell Science and Innovation Campus, Didcot, Oxon OX11 0FA, UK

* Corresponding author: vesna.middelkoop@vito.be

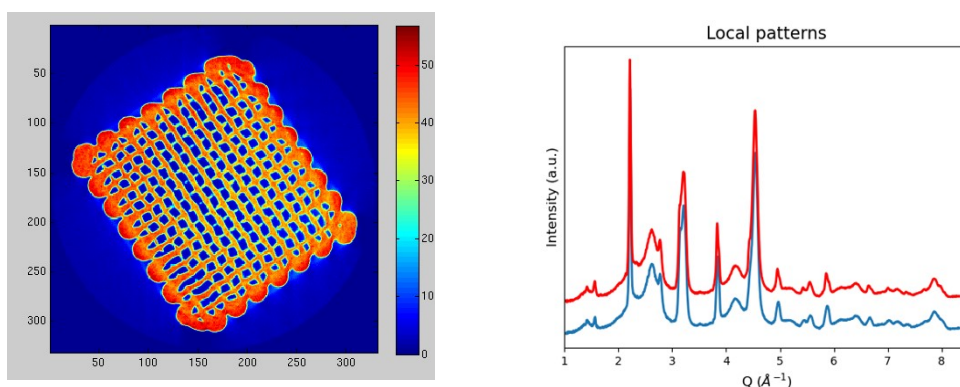


Figure S1. Synchrotron XRD-CT data (before the conventional or DLSR reconstruction was used) showing a complete slice (left); two mean diffraction patterns selected from two typical pixels within the sample.

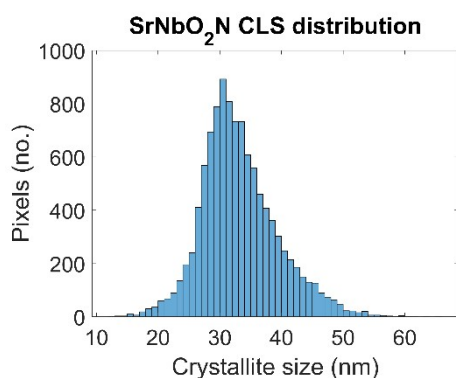


Figure S2. Crystallite size distribution estimated from the CLS maps (XRD peak width analysis of each individual pixel) using the Scherrer equation.

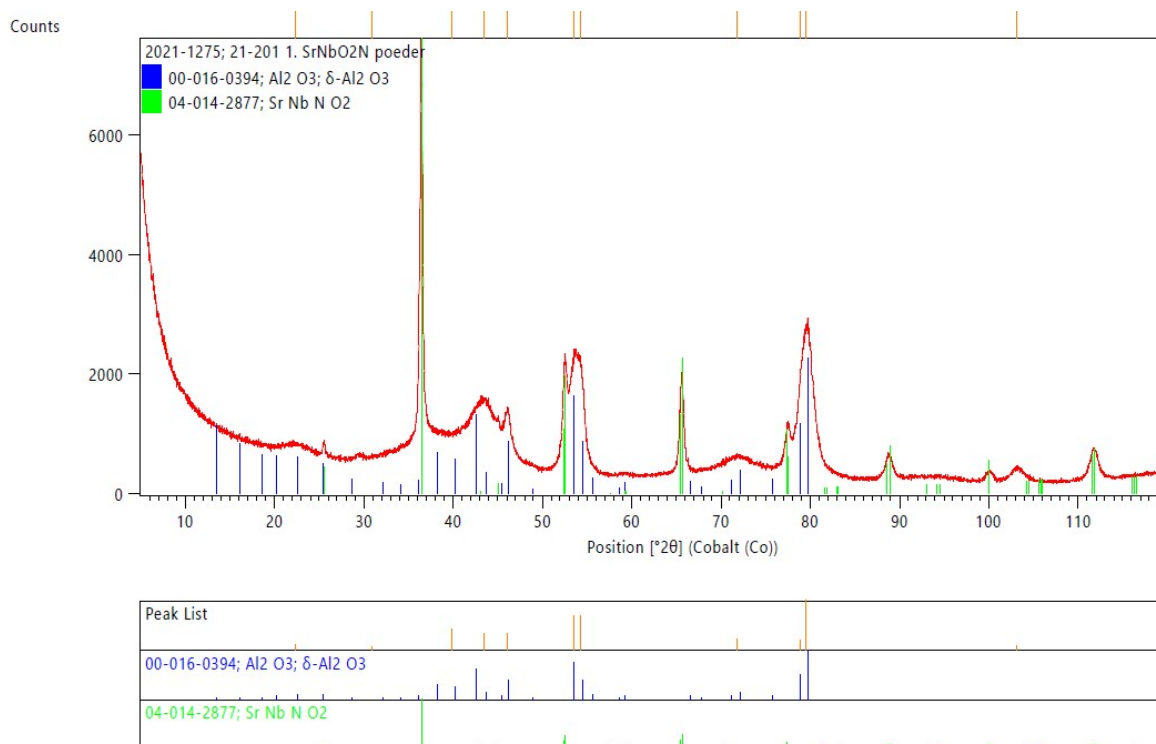


Figure S3. XRD pattern of the starting as-synthesised SrNbO₂N powder.

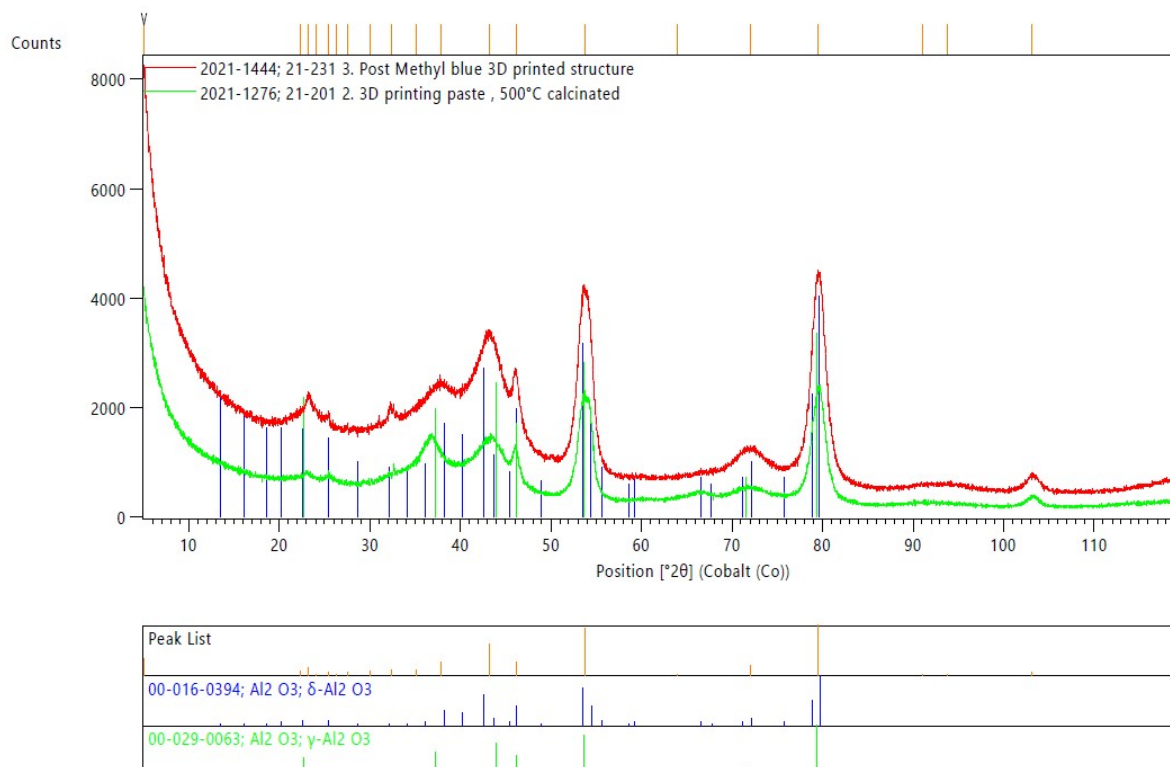


Figure S4. XRD pattern of the 3D printing SrNbO₂N ink (paste) and 3D printed SrNbO₂N structure after photocatalytic testing.

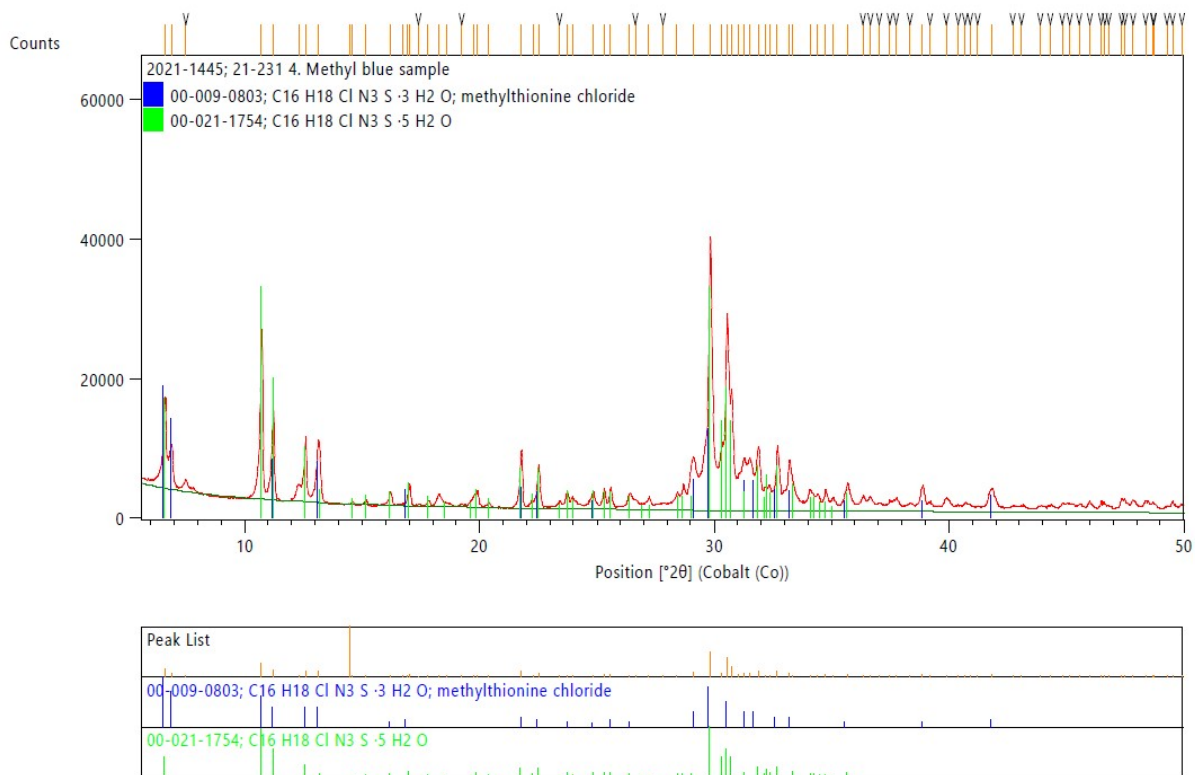


Figure S5. XRD pattern of the Methylene blue sample.

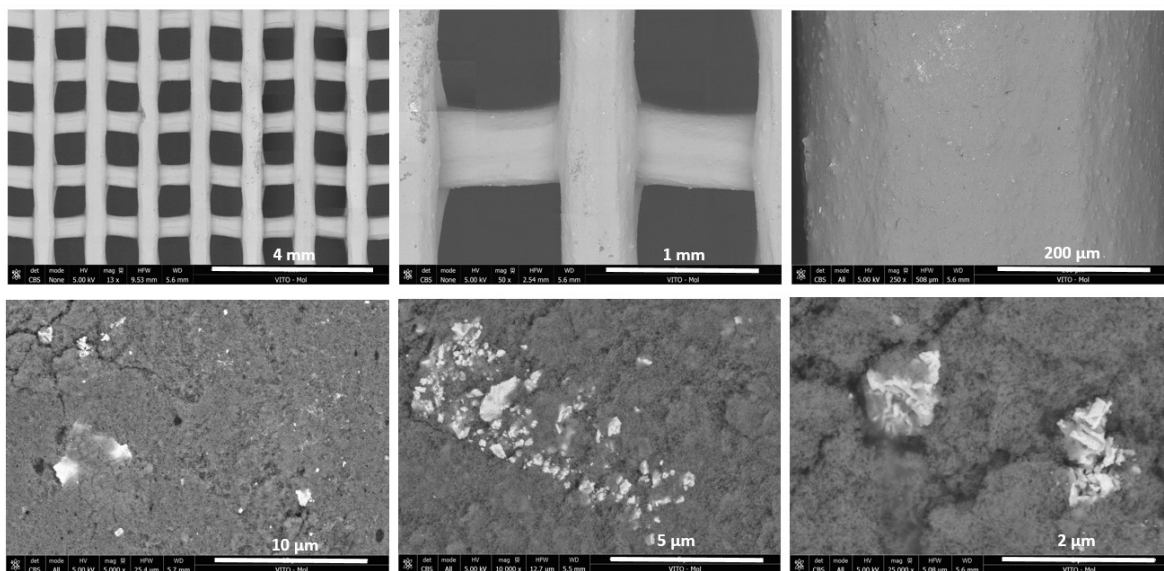


Figure S6. Top row: SEM images of the macrostructure of the 3D printed photocatalyst; bottom row: selected regions of interest (ROIs) revealing the morphology of the individual grains of the photocatalytically active SrNbO₂N phase across the alumina support at different magnifications: 13x, 50x, 250x in the top row, 5000x, 10000x, 25000x in the bottom row, viewed from left to right.

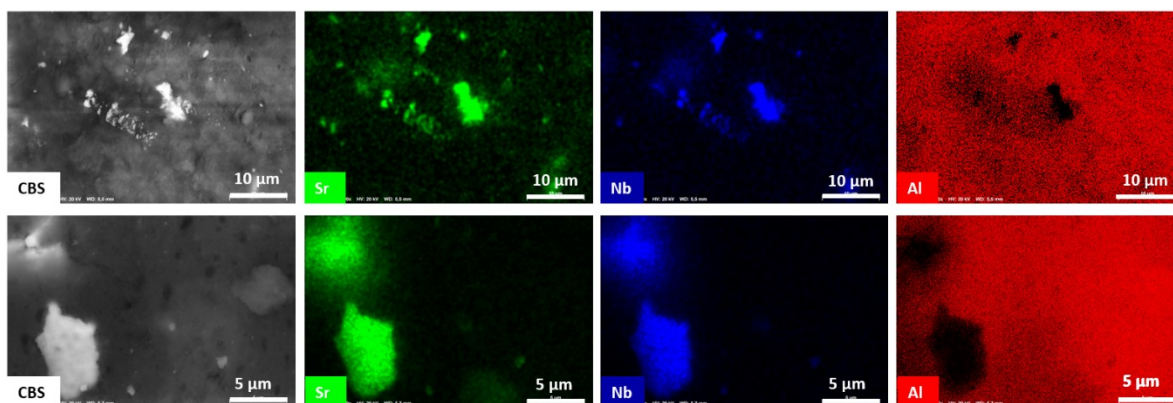


Figure S7. Selected ROI: concentric backscatter (CBS) imaging (an imaging modality available in SEM); EDX maps revealing the distribution of active SrNb-containing phase across the alumina support of the 3D printed photocatalyst (viewed from left to right; 10 μm scale bar in the top row and 5 μm scale bar in the bottom row).

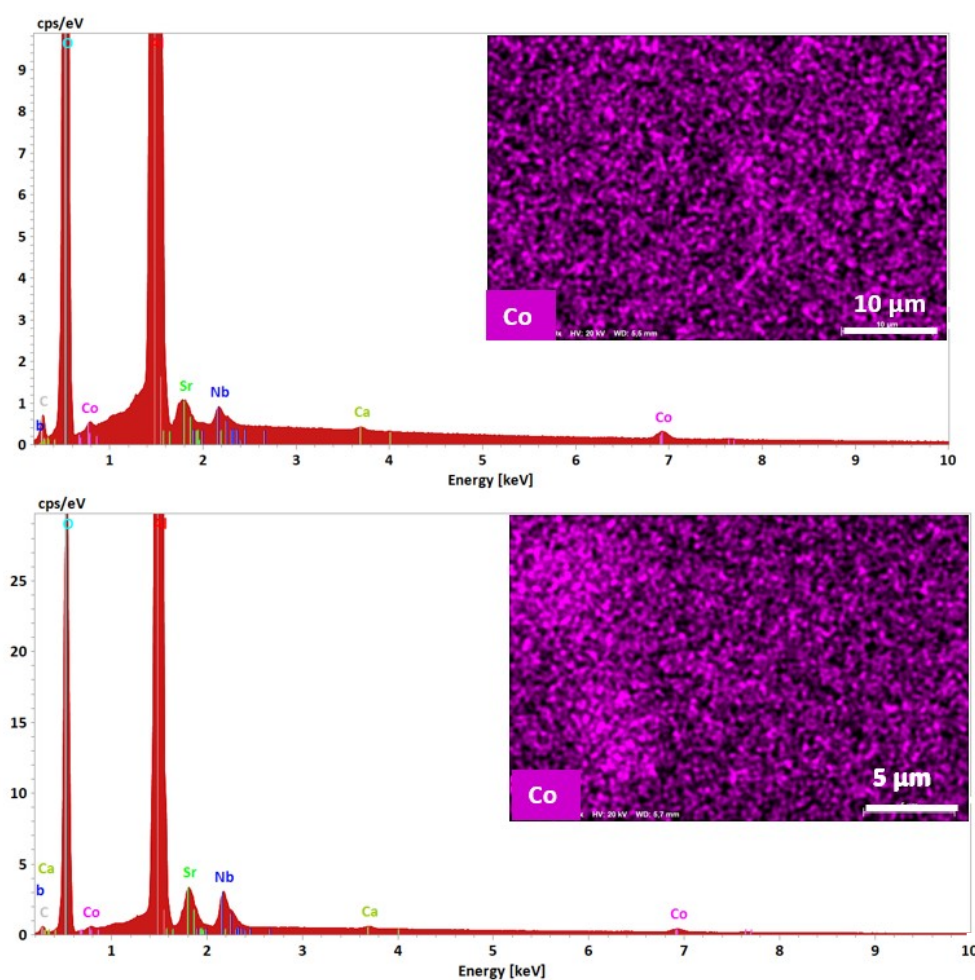


Figure S8. Selected ROI as in Figure S7: EDX spectra showing low concentrations of Cobalt detected. Corresponding EDX maps revealing the distribution (small features) of Cobalt oxide, when used as a co-catalyst deposited across the 3D printed monolith (10 μm scale bar in the top row and 5 μm scale bar in the bottom row).

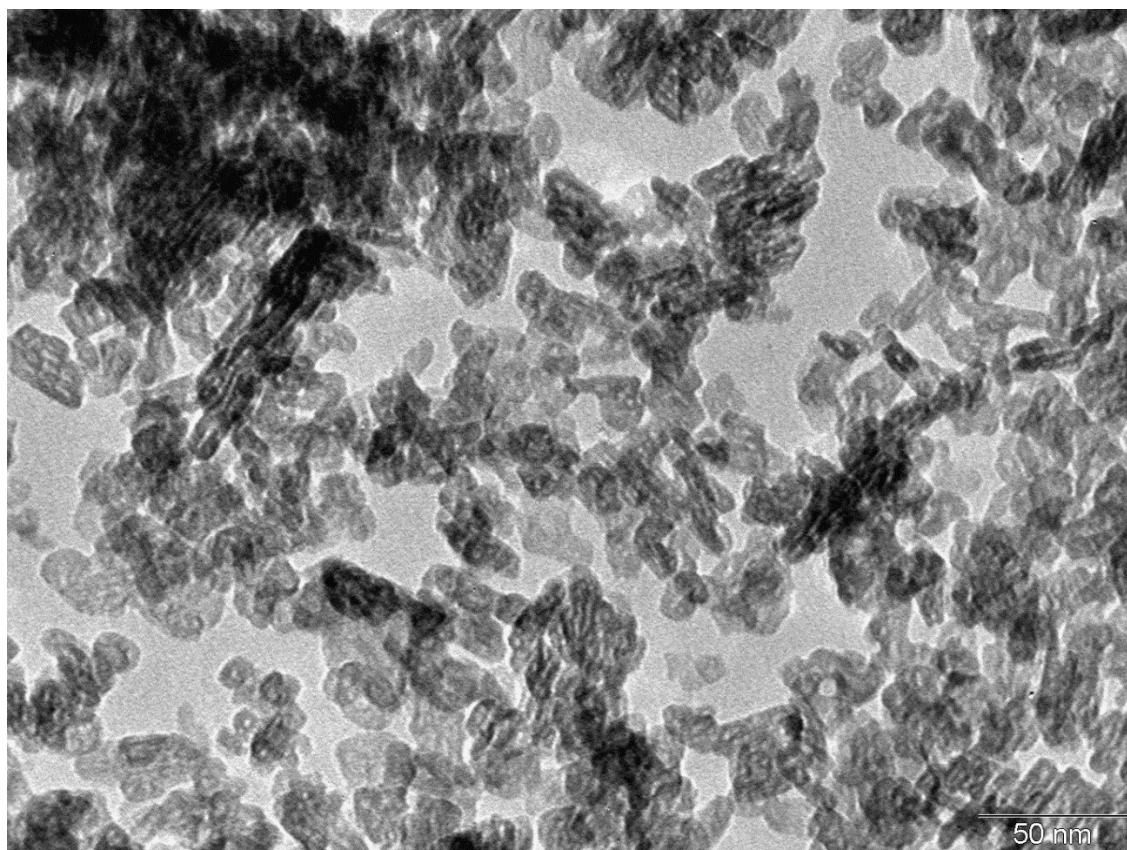


Figure S9. TEM image of the photocatalyst nanoparticles of the starting SrNbO_2N powder (scale bar is 50 nm).

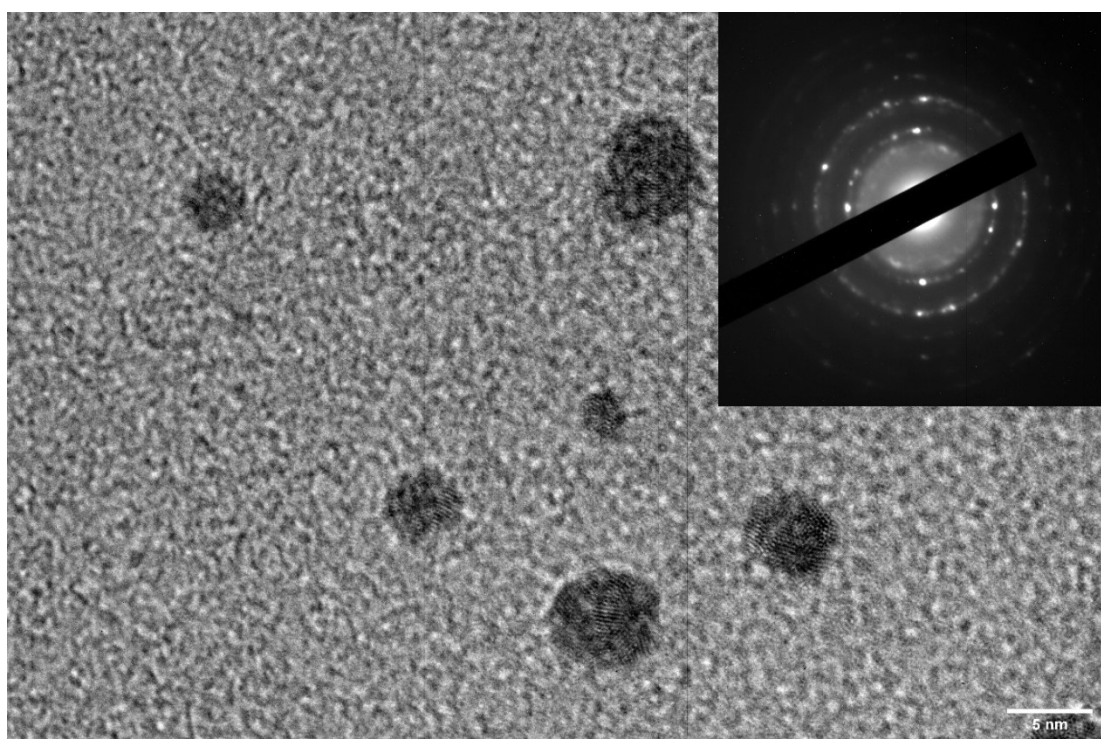


Figure S10. HRTEM image of the photocatalyst particles of the 3D printed monolith material after the degradation tests (scale bar is 5 nm) and the corresponding selected area electron diffraction (SAED) pattern (inset).

The BET surface area of the 3D printed monolith material after the degradation tests was found to be 131.4 m²/g.

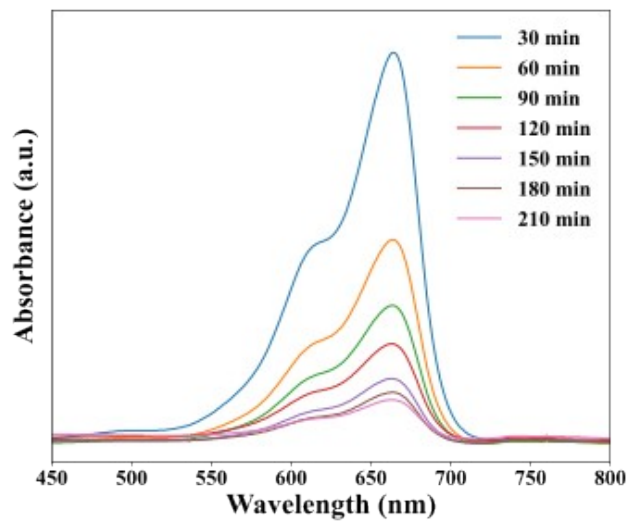


Figure S11. The absorption spectra of MB degradation in the presence of the catalyst.

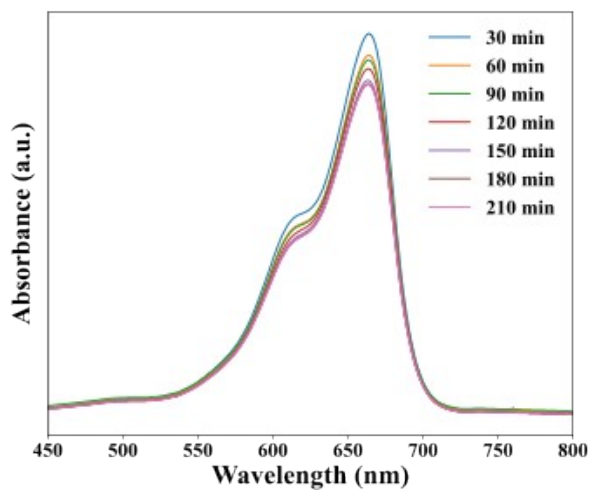


Figure S12. Photocatalytic degradation of MB under light in the absence of catalyst.

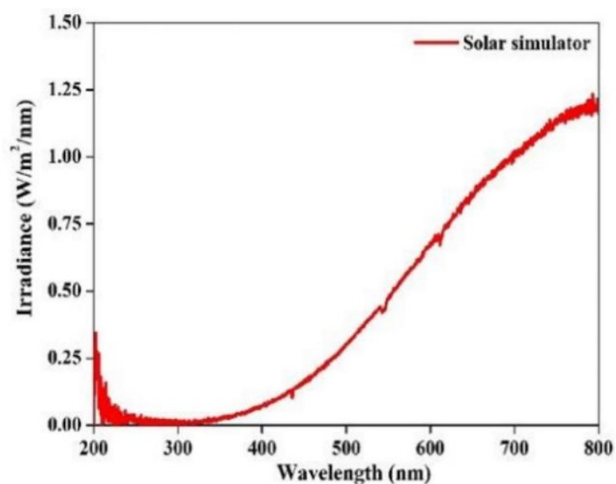


Figure S13. Irradiance curve (irradiance readings as a function of wavelength) for the light source used in the experiments shown Figures 4, 5 and 6 in the Main Manuscript.

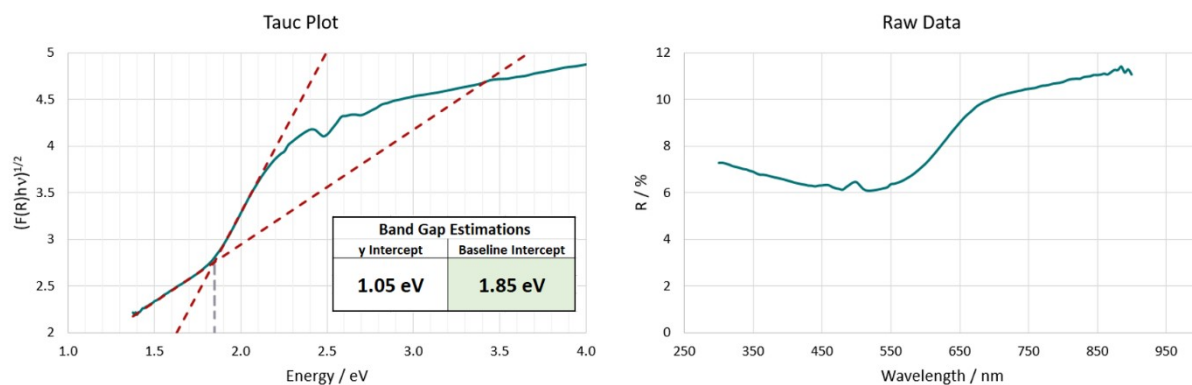


Figure S14. Band-gap extraction for the SrNbO₂N photocatalyst using Tauc-plot: the Tauc plot (left) constructed from the collected raw diffuse reflectance data (right). The red dashed lines represent linear fits to the region and estimates of the band-gap from the intercept.

The average lifetime was determined from the amplitude weighted average of fitted exponentials using equation S1:

$$\tau_{avg} = \frac{a_1\tau_1 + a_2\tau_2 + a_3\tau_3}{a_1 + a_2 + a_3} \quad (\text{Equation S1})$$

where a_1, a_2, a_3 are pre-exponential factors and τ_1, τ_2, τ_3 are the lifetimes of the fitted components.

Table S1. Fitting parameters of PL decays of the samples studied. The average lifetime was determined using Equation S1.

Sample	a_1	τ_1 (ns)	a_2	τ_2 (ns)	a_3	T_3 (ns)	T_{avg} (ns)
3D structure without MB	0.29	1.7	0.55	5.3	0.16	16.2	6.0
3D structure with MB after 1 st photocatalytic activity	0.49	0.5	0.30	2.3	0.21	8.2	2.6

(Experiment 1)							
3D structure with MB after 2 nd photocatalytic activity (Experiment 2)	0.69	1.7	0.29	3.6	0.02	7.8	2.4
3D structure with MB after 3 rd photocatalytic activity (Experiment 3)	0.51	0.3	0.36	2.0	0.13	8.5	2.0
3D structure with MB after 4 th photocatalytic activity (Experiment 4)	0.68	0.44	0.26	3.1	0.06	14.4	2.0
3D structure with MB after 5 th photocatalytic activity (Experiment 5)	0.73	0.47	0.27	4.3	0	0	1.5